Supplementary Information (SI) for New Journal of Chemistry.
This journal is © The Royal Society of Chemistry and the Centre National de la Recherche Scientifique 2024

Electronic Supporting Information

Pathway complexity in aqueous J-aggregation of an ionic BODIPY amphiphile

Houchen Wang,[‡ab] Jiajun Liu,[‡a] Hongfei Pan,[a] and Zhijian Chen*[a]

[a] *School of Chemical Engineering and Technology, Tianjin University, Tianjin, 300072, China.*
[b] *College of Chemistry, Chemical Engineering and Materials Science, Zaozhuang University, Zaozhuang, 277160, China.*

[‡]These authors contributed equally to this work.

E-mail: zjchen@tju.edu.cn

Table of Contents

1. Materials and Methods

Chemicals and reagents: All the chemicals used were analytical grade and were used without further purification unless otherwise stated. CH_2Cl_2 was distilled over CaH_2 under Ar, and tetrahydrofuran (THF) was distilled over sodium and stored under Ar. Silica gel (200-300 mesh) was used for column chromatography.

NMR spectroscopy: ^{1}H and ^{13}C NMR spectra were recorded on Bruker AVANCE III HD (400 MHz) spectrometer using tetramethylsilane (TMS) as internal standard.

Mass spectrometry: High resolution mass spectrum (ESI) was measured with a Bruker miorOTOF-QII mass spectrometer.

UV/Vis spectroscopy: UV/Vis absorption spectra were recorded by using a UV/Vis spectrophotometer (Agilent Technologies, Cary 300) equipped with a SPV temperature controller. The solvents for spectroscopic studies were spectroscopic grade and deionized H_2O were used as received, and all the UV/V spectra were corrected by the blank solution. The quartz glass cuvettes were used to measurement and the extinction coefficients ε were calculated according to Lambert-Beer's law: $A = \varepsilon bc$.[1]

Fluorescence spectroscopy: The steady state fluorescence spectra, fluorescence quantum yields, and fluorescence lifetimes were measured on a FLS980 spectrofluorometer (Edinburgh). All of the fluorescence spectra were corrected. For the samples of dye aggregates, the measurements were performed by using a front-face setup to minimize reabsorption. Fluorescence quantum yields were determined under ambient conditions by the integrating sphere on the spectrofluorometer. Fluorescence lifetime measurements were performed on a time-correlated single-photon counting (TCSPC) setup. A nF920 nanosecond flashlamp (pulse width <1 ns) was used as excitation source (200 - 400 nm). A RED PMT photomultiplier (R928P) was used as detector. The instrument response was collected by scattering the excited light of a dilute, aqueous suspension of colloidal silica (Ludox). The lifetime decay curves were analyzed using the software supplied with the instrument. The quality of the data fitting was evaluated by analysis of χ^2 (0.9−1.1) as well as by inspection of residuals and the autocorrelation function.

Transmission electron microscopy (TEM): The TEM measurements were recorded on a JEM-2100F transmission electron microscope. For sample preparation, a drop of aggregates in solution of dye **3** was placed on 400-mesh formvar copper grids coated with carbon. About 2 min after the deposition, the grid was blotted with filter paper to remove solvent. Staining was performed by addition of a drop of uranyl acetate aqueous solution (0.5 %) onto the copper grid. After 1 min, the surface liquid on the grid was removed with filter paper.

Atomic force microscopy (AFM): The AFM measurements were performed under ambient conditions using a Bruker Dimension Icon atomic force microscope operating in tapping mode. Silicon cantilevers with a resonance frequency of ~300 kHz were used. The samples of **Agg. I** and **Agg. II** were prepared by drop-casting the solution of dye aggregates (2.0×10^{-5} M) in H_2O on mica sheets.

Dynamic light scattering (DLS) and zeta potential: The particle size distribution and zeta potential values of dye aggregates in the aqueous solution were measured by a Zetasizer Nano ZS Nanoparticle Size and Zeta Potential Analyzer (4 mW 633 nm helium-neon laser) manufactured by Malvern.

XRD measurement: One-dimensional XRD measurement was performed on a Rigaku Smartlab diffractometer with Cu Kα source operating at 45 kV and 200 mA. The experiments were performed at a sample-detector distance of 21 cm, with the detector tilted by 14° upward in order to study the angular range of $2\theta = 0.5°$-$25°$. The samples were prepared by evaporation of the concentrated **Agg. I** and **Agg. II** solution in H_2O on glass slide.

2. Synthesis and characterization

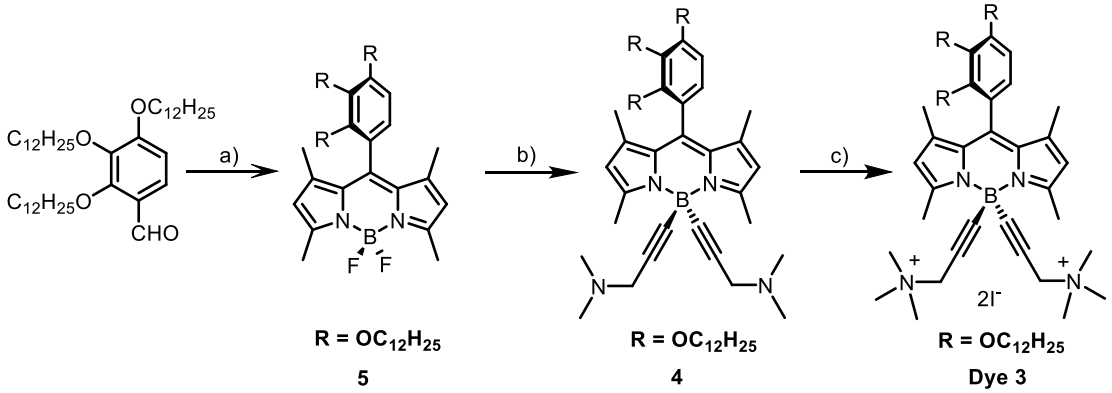

Scheme 1 Synthesis of amphiphile BODIPY dye **3**. Reagents and conditions: a) CF_3COOH, 2,4-Dimethylpyrrole, CH_2Cl_2, r.t., 30min; DDQ, 30 min; DIEA, BF_3•Et_2O, 2 h; b) EtMgBr, THF, 1-dimethylamino-2-propyne, 60 ºC, 0.5 h; c) Et_2O, CH_3I, 20 h.

Compound 5: 2,3,4-tris(dodecyloxy)benzaldehyde (2.63 g, 4 mmol, 1 eq) and 2,4-dimethylpyrrole (0.84 g, 8.84 mmol, 2.21 eq) were dissolved in dry CH_2Cl_2 (50 mL) under Ar. After 5 min, TFA (0.10 mL) was added, and the reaction was continued at room temperature for about another 15 min. After the complete consumption of aldehyde (monitored by TLC), DDQ (0.95 g, 4 mmol, 1 eq) was added into the reaction mixture. Then the reaction was continued for 0.5 h, N, N-Diisopropylethylamine (7 mL) and $BF_3 \cdot Et_2O$ (7 mL) were added subsequently. The reaction mixture was carried out at room temperature for 2 h. Then the solvent was evaporated under reduced pressure and the residue was purified by column chromatography (silica gel, CH_2Cl_2/*n*-Hexane= 1/1, v/v) to give an orange-colored substance **3-1** (1.21 g, Y = 34.47%). ^{1}H NMR (400 MHz, $CDCl_3$): δ = 6.77 (d, *J* = 8.5 Hz, 1H), 6.72 (d, *J* = 8.5 Hz, 1H), 5.95 (s, 2H), 3.97 (m, 6.4 Hz, 6H), 2.54 (s, 6H), 1.91 - 1.80 (m, 2H), 1.80 - 1.70 (m, 2H), 1.54 (s, 6H), 1.44 - 1.00 (m, 56H), 0.88 (t, 9H).^{13}C NMR (101 MHz, $CDCl_3$): δ = 154.79, 154.52, 150.62, 142.55, 142.37, 132.08, 123.42, 121.42, 120.82, 108.56, 77.33, 77.01, 76.69, 73.59, 68.84, 31.94, 30.34, 30.29, 29.70, 29.64, 29.57, 29.48, 29.38, 26.15, 25.74, 22.70, 14.57, 14.21, 14.11.

Compound 4: To a solution of 1-dimethylamino-2-propyne (0.56 g, 4.34 mmol, 8.5 eq) in dry THF (4 mL) under Ar in a flask, EtMgBr (1.0 M in THF, 4.08 mL, 4.08 mmol, 8 eq) was added and the mixture was stirred at 55 °C for 2 h. Compound **5** (0.45 g, 0.51 mmol, 1 eq) was dissolved in dry THF (2 mL) under Ar, and then the solution of the Grignard reagent was transferred via a cannula to the solution of BODIPY **5**. After the reaction was complete monitored by TLC, H_2O (30 mL) was added. The mixture was extracted with CH_2Cl_2 (20 mL × 3), dried by Na_2SO_4, and then concentrated in vacuo. The residue was purified by column chromatography (silica gel, CH_2Cl_2/MeOH = 3/1, v/v) to give a dark-orange solid (0.38 g, Y = 74.51%). ^{1}H NMR (400 MHz, $CDCl_3$): δ = 6.80 (d, *J* = 8.5 Hz, 1H), 6.72 (d, *J* = 8.5 Hz, 1H), 5.99 (s, 2H), 3.97 (m, 6H), 3.27 (d, *J* = 3.1 Hz, 4H), 2.76 (s, 6H), 2.33 (d, *J* = 13.8 Hz, 12H), 1.90 - 1.81 (m, 2H), 1.79 - 1.69 (m, 2H),

1.54 (s, 6H), 1.43 - 0.99 (m, 56H), 0.88 (t, J = 6.7 Hz, 9H). ^{13}C NMR (101 MHz, $CDCl_3$): δ = 154.56, 154.50, 150.93, 146.01, 142.36, 140.57, 138.85, 130.37, 123.83, 122.06, 121.30, 108.55, 77.54, 77.28, 77.03, 73.77, 68.98, 49.17, 49.06, 44.33, 44.25, 44.05, 32.18, 32.17, 30.55, 30.39, 30.02, 29.98, 29.97, 29.95, 29.93, 29.91, 29.88, 29.81, 29.76, 29.72, 29.64, 29.63, 29.62, 29.60, 26.39, 25.90, 22.94, 16.41, 14.68, 14.37.

Dye 3: Compound **4** (0.30 g, 0.30 mmol, 1 eq) was stirred in dry diethyl ether, and then iodomethane (0.43 g, 3.00 mmol, 10 eq) was added to the mixture in dark at 30 °C. The stirring was continued for overnight. After the reaction was complete, the precipitated solid was isolated by filtration, and then washed by diethyl ether. The compound was recrystallized by CH_2Cl_2 and Et_2O, and obtained orange colored powder (0.29 g, Y = 74.36%). ^{1}H NMR (400 MHz, $CDCl_3$): δ = 6.82 (d, J = 8.5 Hz, 1H), 6.75 (d, J = 8.7 Hz, 1H), 6.09 (s, 2H), 4.72 (d, J = 29.8 Hz, 4H), 4.02 (t, J = 6.2 Hz, 2H), 3.99 - 3.89 (m, 4H), 3.51 (d, J = 3.7 Hz, 18H), 2.73 (s, 6H), 1.90 - 1.82 (m, 2H), 1.78 - 1.72 (m, 2H), 1.55 (d, J = 13.3 Hz, 6H), 1.51 - 1.01 (m, 56H), 0.88 (dd, J = 7.3, 5.4 Hz, 9H).^{13}C NMR (101 MHz, [D_6]DMSO): δ = 154.61, 154.54, 153.84, 150.07, 147.17, 142.07, 141.39, 140.97, 139.55, 135.95, 130.11, 124.97, 123.73, 122.84, 122.20, 120.73, 73.17, 56.72, 52.34, 52.15, 40.66, 40.45, 40.24, 40.03, 39.83, 39.62, 39.41, 31.81, 30.22, 29.89, 29.59, 29.56, 29.48, 29.42, 29.34, 29.27, 29.24, 28.92, 26.22, 26.08, 25.49, 22.58, 16.28, 14.40, 14.38, 14.35. HRMS (ESI, positive mode): calculated for $C_{67}H_{113}BN_4O_3^{2+}$ 1032.8895, found: m/z $[M]^{2+}$ 516.4469. UV/Vis (CH_2Cl_2): λ_{max} (ε) = 504 nm (9.15×10^{-5} M^{-1} cm^{-1}). Fluorescence (CH_2Cl_2): λ_{max} = 521 nm; quantum yield: $\Phi_{monomer}$ = 32.71% (CH_2Cl_2), lifetime: $\tau_{monomer}$ = 3.1 (CH_2Cl_2).

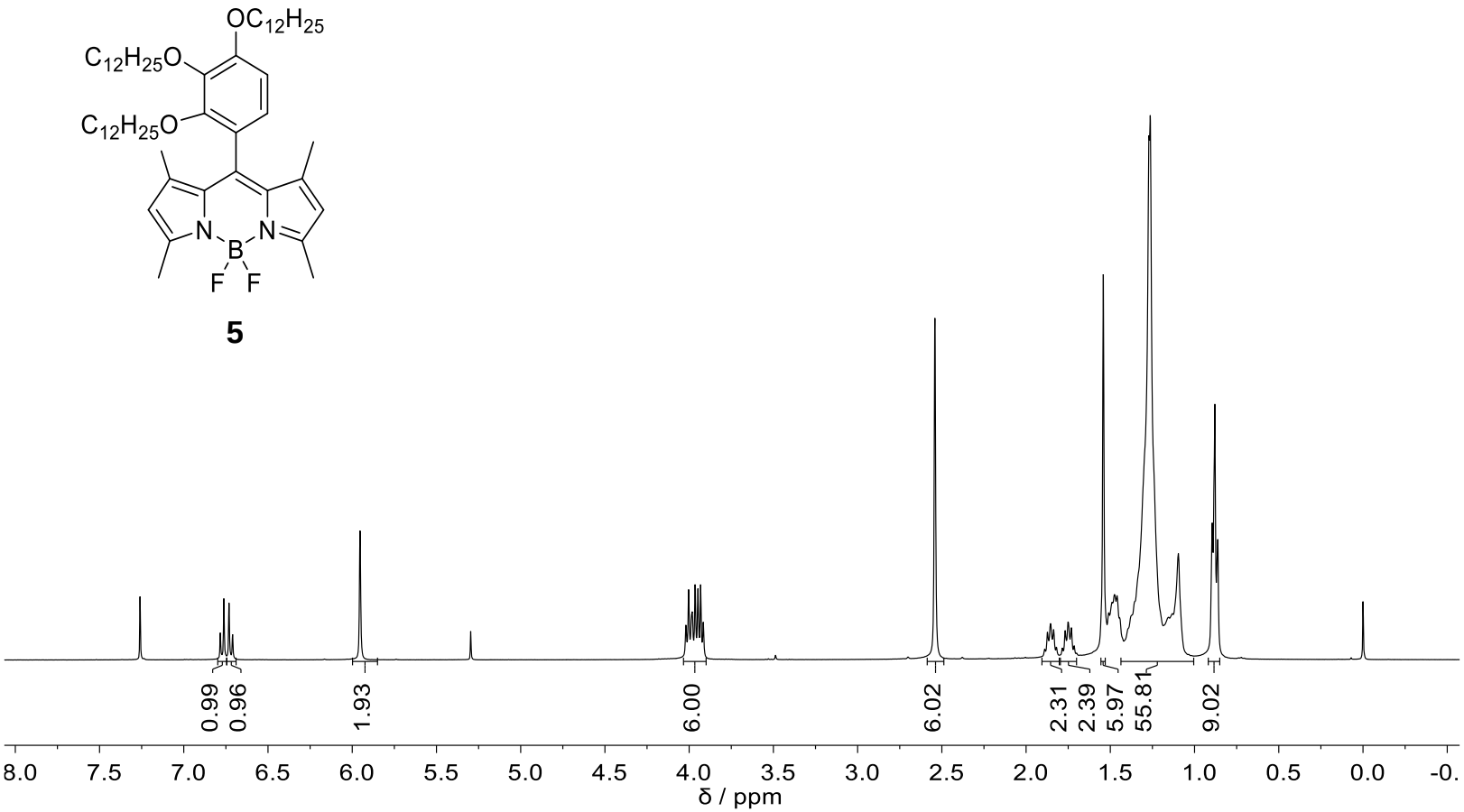

Fig. S1 The ^{1}H NMR spectrum (400 MHz) with chemical molecular structure of compound **5** in $CDCl_3$ at 293 K.

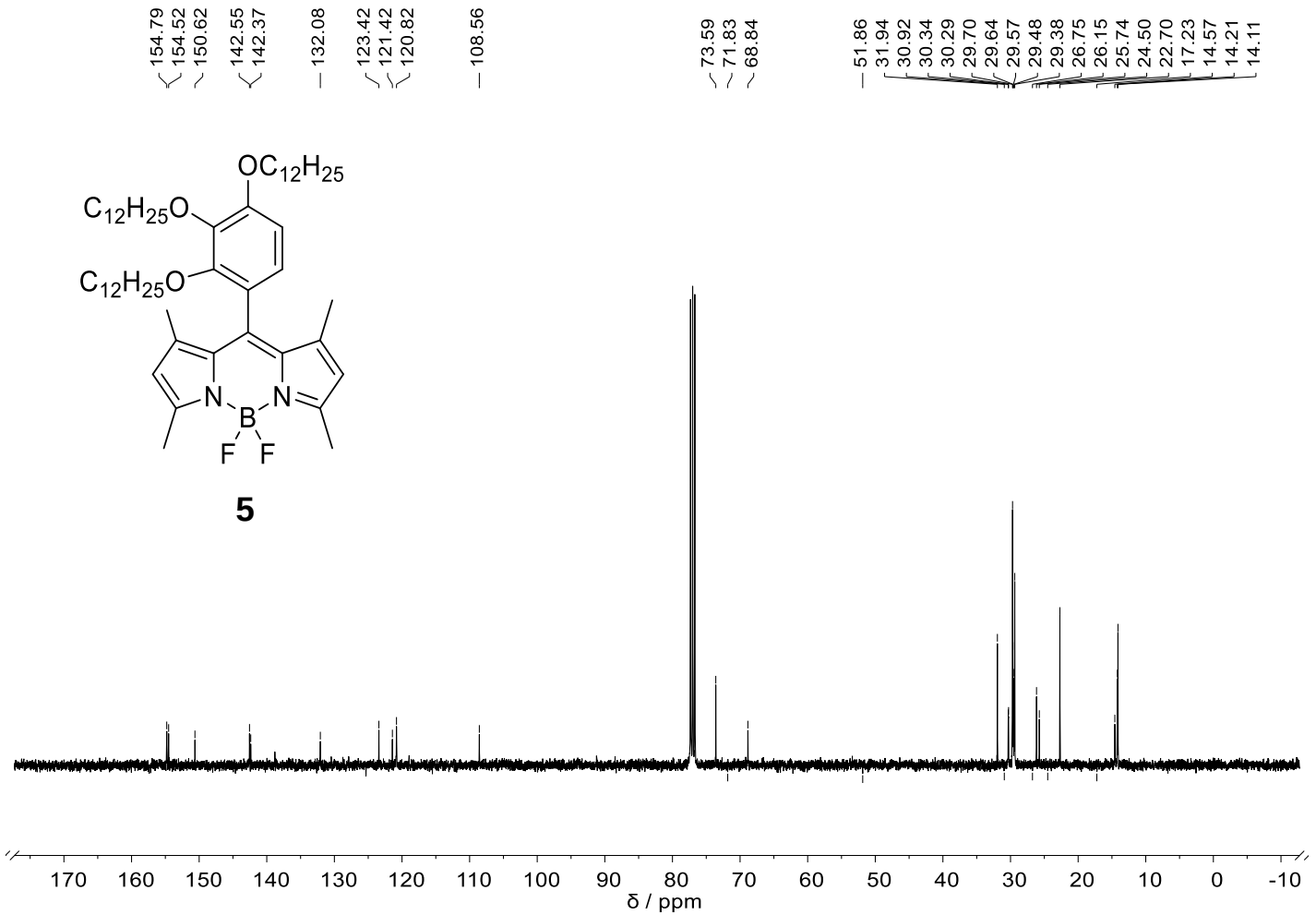

Fig. S2 The ^{13}C NMR spectrum (101 MHz) of compound **5** in $CDCl_3$ at 293 K.

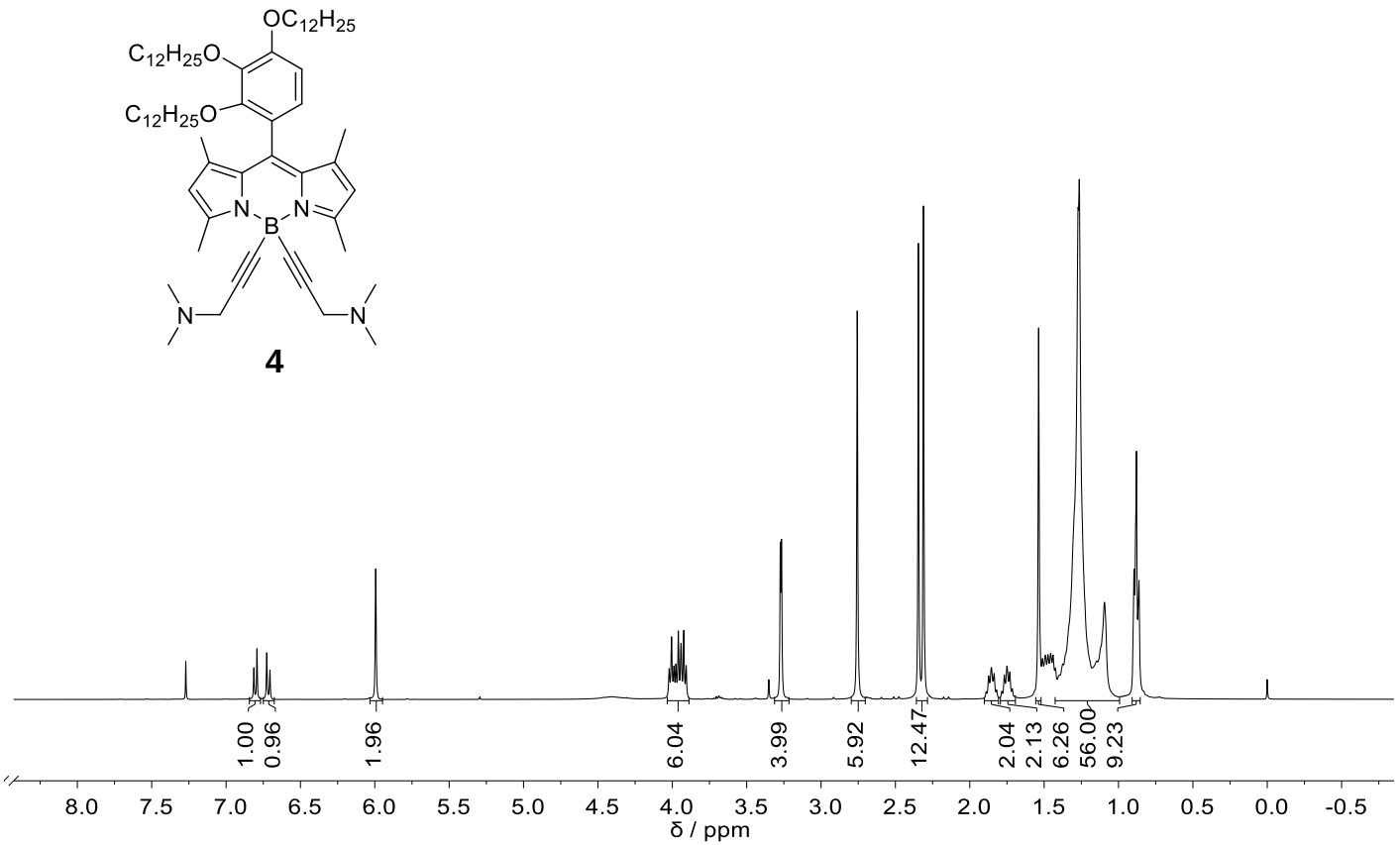

Fig. S3 The ^{1}H NMR spectrum (400 MHz) with corresponding assignments of compound **4** in $CDCl_3$ at 293 K.

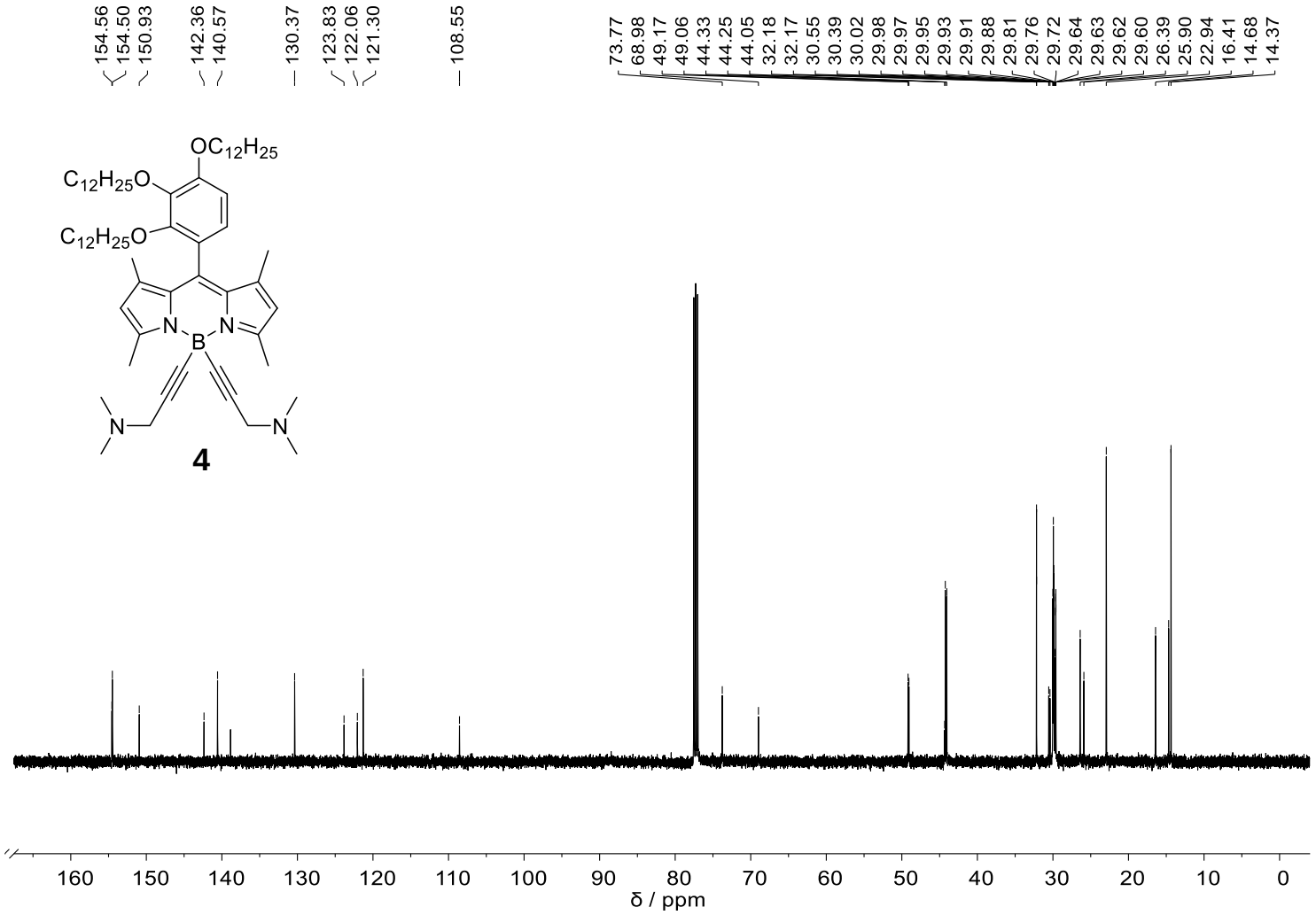

Fig. S4 The ^{13}C NMR spectrum (101 MHz) of compound **4** in $CDCl_3$ at 293 K.

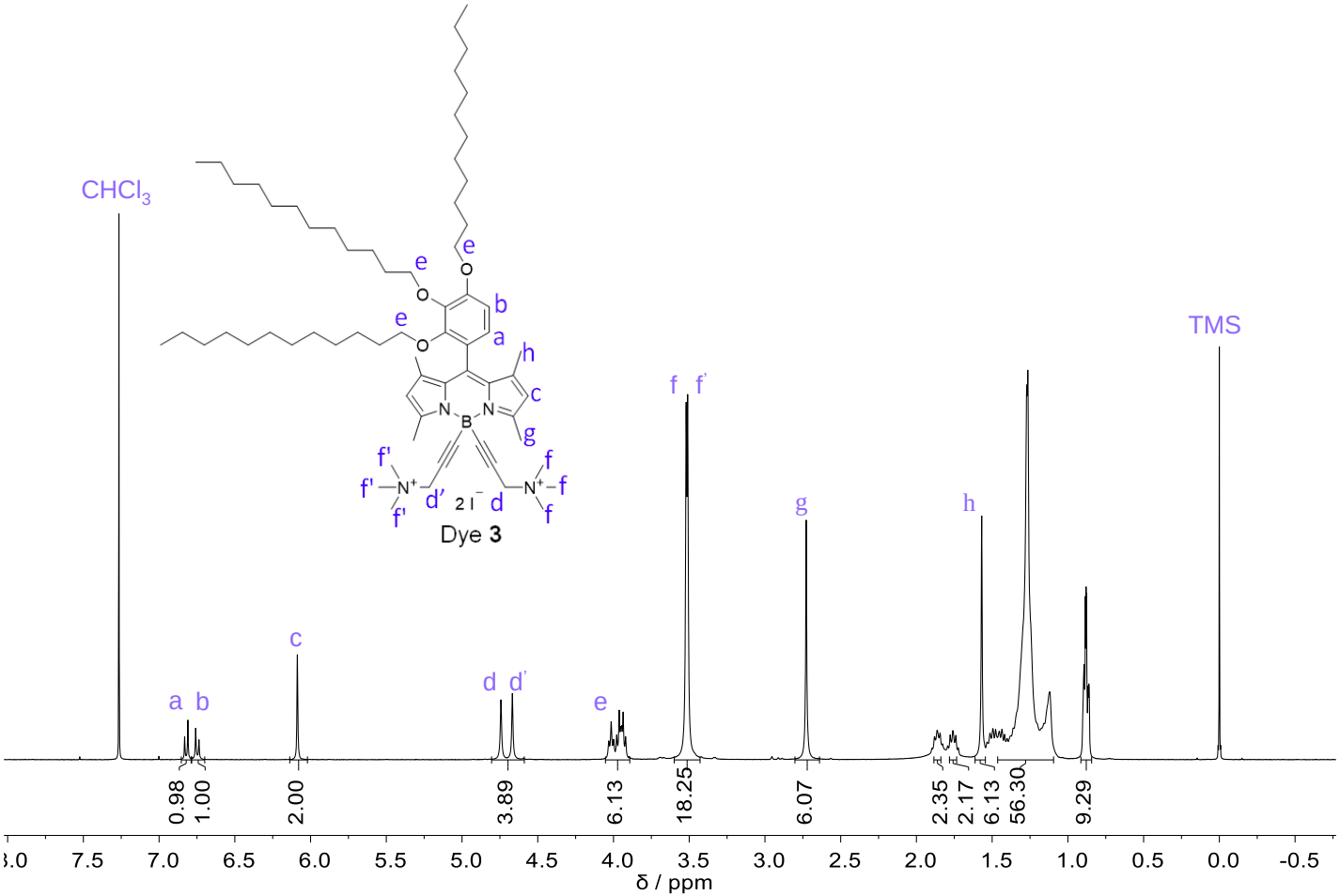

Fig. S5 The ^{1}H NMR spectrum (400 MHz) with corresponding assignments of dye **3** in $CDCl_3$ at 293 K.

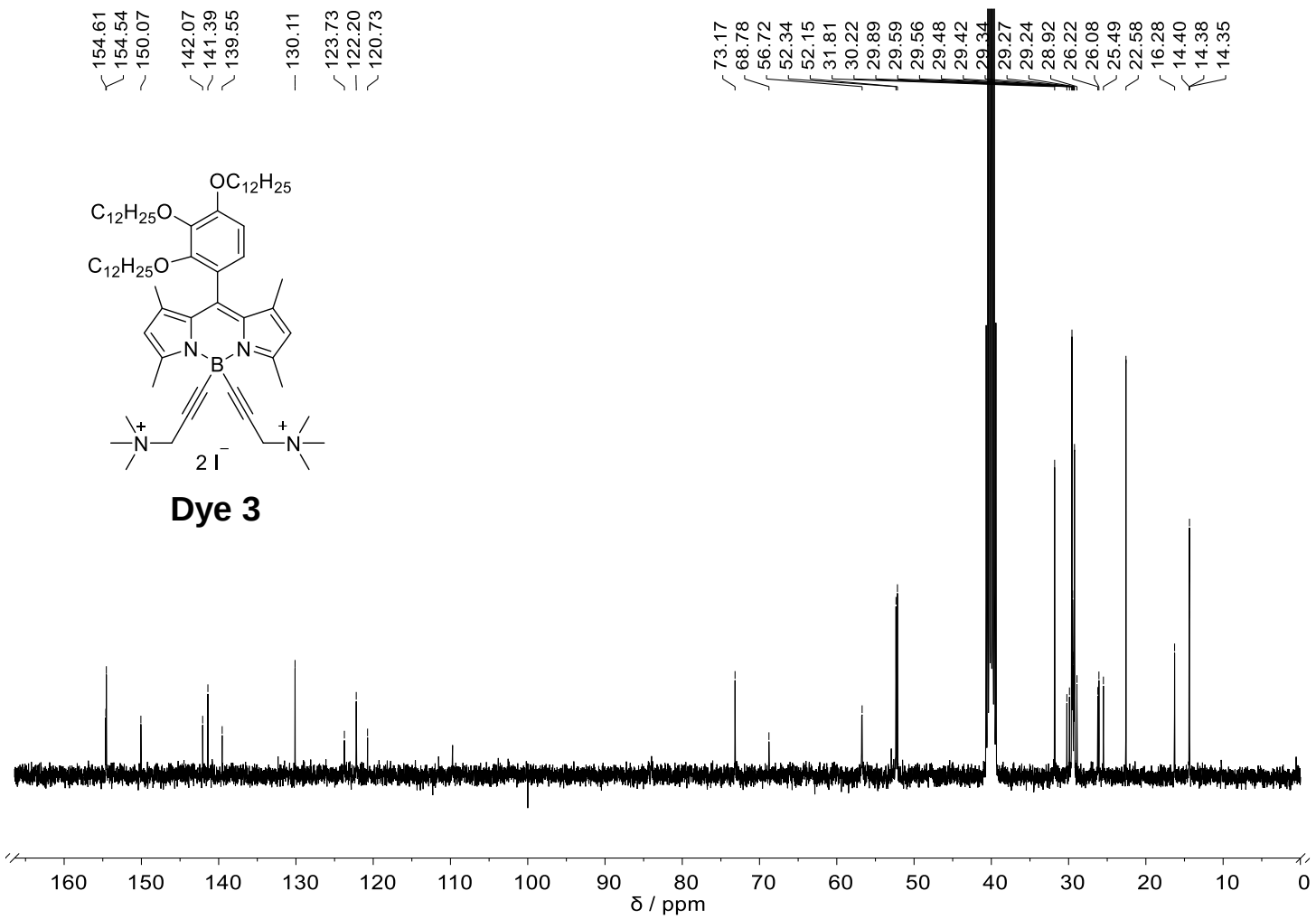

Fig. S6 The ^{13}C NMR spectrum (101 MHz) of dye **3** in [D_6] DMSO at 293 K.

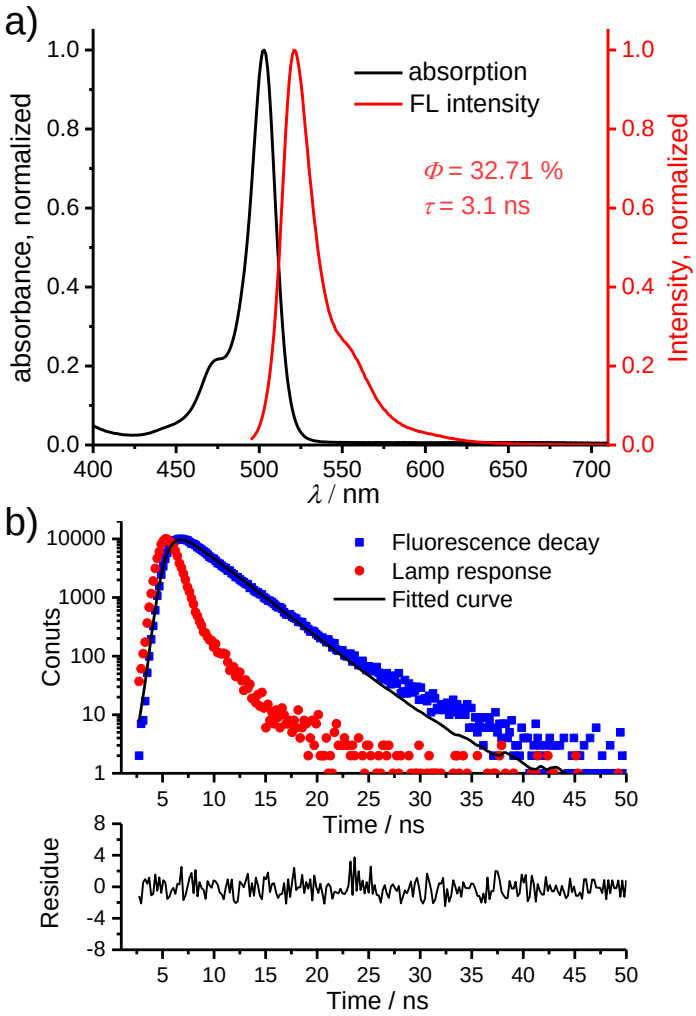

Fig. S7 a) UV/Vis absorption (black line) and fluorescence spectrum (red line) of dye **3** in CH_2Cl_2 (1.0×10^{-6} M, λ_{ex} = 480 nm). b) Fluorescence lifetime of monomer of dye **3** in CH_2Cl_2 ($c_T = 1\times10^{-6}$ M) at 293 K. The curves were fitted with single-exponential decay function. λ_{ex} = 366 nm, λ_{em} = 521 nm. τ_{Mon} = 3.1 ns, χ^2 = 1.038.

3. Data analysis for spectroscopic studies

Temperature-dependent spectroscopic measurements

The temperature-dependent spectroscopic data were evaluated by the nucleation-elongation model proposed by Meijer and coworkers.[2] The fraction of aggregated molecules α_{Agg} at a certain concentration and temperature can be estimated based on the assumption that the dye molecules aggregate fully (α_{Agg} = 1) at lowest temperature (T = 275 K) or highest concentration (c = 5×10^{-4} M) and stay in monomers (α_{Agg} = 0) at highest temperature (T = 333 K) or lowest concentration (c = 5×10^{-7} M) in H_2O, ε_{Mon} and ε_{Agg} stands for absorption coefficients of the monomer and fully aggregated state respectively.

For **Agg. II**, during heating process, where two species, i.e., the monomer and **Agg. II**, are involved, the fraction of aggregated molecules at certain temperature T can be calculated according to Eq. S1:

$$\alpha_{Agg} = 1 - \frac{\varepsilon - \varepsilon_{Agg}}{\varepsilon_{Mon} - \varepsilon_{Agg}} \quad (S1)$$

For the nucleation-growth model, the cooperative aggregation process can be described as two steps: nucleation and elongation. In the elongation regime, the molar fraction of aggregated dye (α_{agg}) can be expressed as equation (S2):

$$\alpha_{Agg} = \alpha_{SAT}\left\{1 - exp\left[\frac{-\Delta H_e}{RT_e^2}(T - T_e)\right]\right\} \quad (S2)$$

Here, ΔH_e is the enthalpy corresponding to elongation regime, T is the temperature, T_e is the elongation temperature, R is the ideal gas constant and α_{SAT} is a parameter introduced to ensure that $\alpha_{agg}/\alpha_{SAT}$ does not exceed unity.

At the temperature above T_e (nucleation regime), the fraction of aggregated molecules in the nucleation regime can be described as equation (S3):

$$\alpha_{Agg} = K_a^{1/3}\exp\left[(2/3K_a^{-1/3} - 1)\frac{\Delta H_e}{RT_e^2}(T - T_e)\right] \quad (S3)$$

In this equation, ΔH_e, T and T_e are the same as equation (S2) and K_a is the dimensionless equilibrium constant of the activation.

The average length of the stack N_n at the T_e is given by equation (S4).

$$N_n(T_e) = \frac{1}{K_a^{1/3}} \quad (S4)$$

Concentration-dependent spectroscopic measurements

The concentration-dependent spectroscopic data were evaluated by the cooperative supramolecular polymerization model proposed by Goldstein and Stryer.[3] In this model, a nucleus of size *s* is formed in the nucleation regime through an isodemic process with an equilibrium constant K_s while further steps of adding more molecules to the nucleus take place with equal equilibrium constant K ($K > K_s$), i.e. $K_1 = K_2 = \bullet\bullet\bullet = K_s$ and $K_{s+1} = K_{s+2} = \bullet\bullet\bullet = K$. The cooperativity is reflected by the parameter σ defined as $\sigma = K_s / K$. The relation between Kc_T and Kc_1 can be described as the equation (S5), where c_1 is the concentration of the monomer species and c_T is the total concentration of the molecules:

$$Kc_T = \sum_{n=1}^{s} n\sigma^{n-1}(Kc_T)^n + \sum_{n=s+1}^{\infty} n\sigma^{s-1}(Kc_T)^n = \frac{s(Kc_1)^s\sigma^{s-1}}{1-Kc_1} + \frac{(Kc_1)^{s+1}\sigma^{s-1}}{(1-Kc_1)^2} + \frac{Kc_1(s(\sigma Kc_1)^{s-1}-1)}{\sigma Kc_1-1} - \frac{\sigma(Kc_1)^2((\sigma Kc_1)^{s-1}-1)}{(\sigma Kc_1-1)^2} - \frac{\sigma(Kc_1)^2((\sigma Kc_1)^{s-1}-1)}{(\sigma Kc_1-1)^2} \quad \text{(S5)}$$

In the meantime, $\alpha_{\text{Agg. II}}$ can be calculated from equation (S6):

$$\alpha_{\text{Agg. II}} = 1 - \alpha_{\text{Mon}} = 1 - \frac{Kc_1}{Kc_T} \quad \text{(S6)}$$

Both $\alpha_{\text{Agg. II}}$ and Kc_T can be obtained from the data of Kc_1 and the curve of $\alpha_{\text{Agg. II}}$ against Kc_T can be drawn. The experiment data from three different wavelengths were collected and manually fitted into the curve for the best match, the result presented in the paper was the average value.

4. Aggregation studies

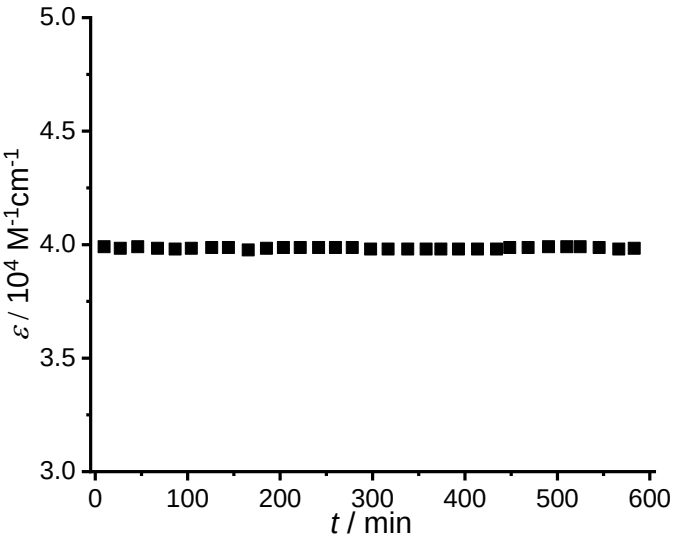

Fig. S8 Time-dependent UV/Vis absorption spectral changes in ε of **Agg. I** in H_2O (2.0×10^{-5} M) monitored at wavelength of 520 nm at 275 K.

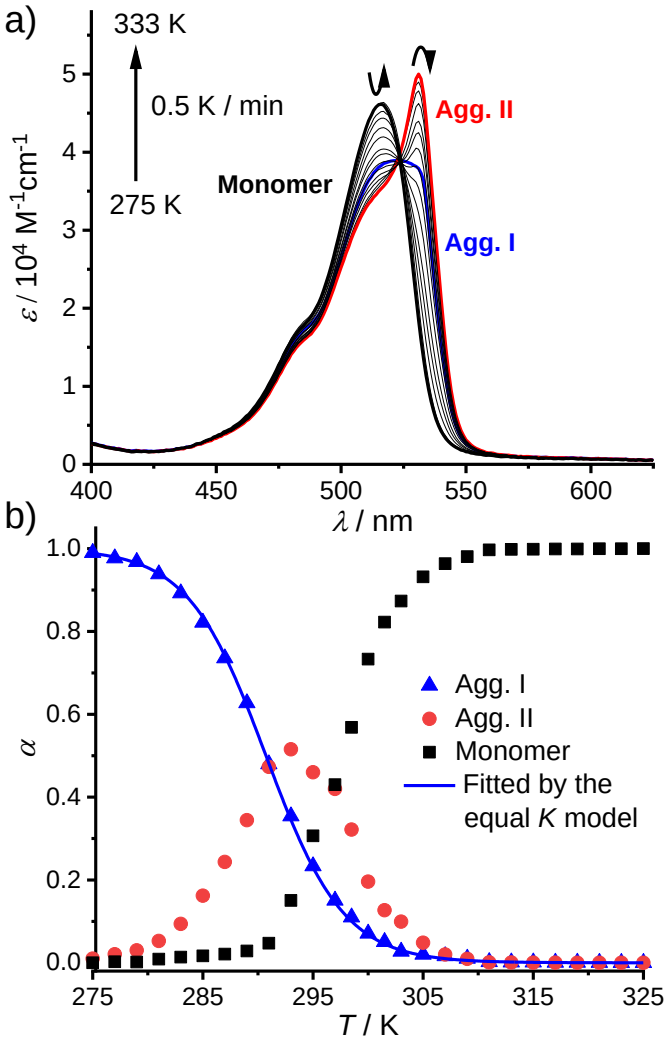

Fig. S9 a) Temperature-dependent UV/Vis absorption spectra of **Agg. I** (c_T = 2.0 × 10^{-5} M) heating from 275 K to 333 K at 0.5 K min^{-1}. b) Plot of the calculated molar fraction of monomer, **Agg. I** and **Agg. II** in the heating process of **Agg. I** from 275 K to 333 K at 0.5 K min^{-1}, and the fitting curves by the equal K mode. The values of $\alpha_{Agg.\ I}$ and $\alpha_{Agg.\ II}$ were estimated based on the spectral data by the method in our previous work.[4]

.

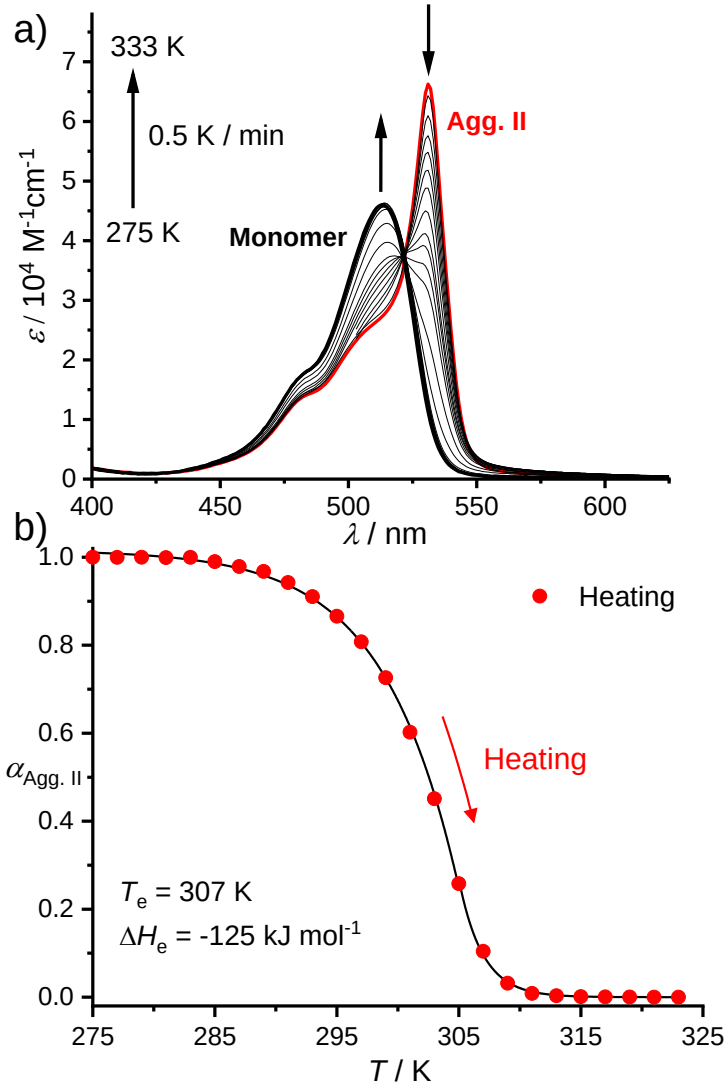

Fig. S10 a) Temperature-dependent UV/Vis absorption spectra of **Agg. II** (c_T = 2.0 × 10^{-5} M) heating from 275 K to 333 K at 0.5 K min^{-1}. b) Plot of the molar fraction of **Agg. II** (c_T = 2.0 × 10^{-5} M) versus temperature for the heating process and the fitting curves by the nucleation-elongation mode.

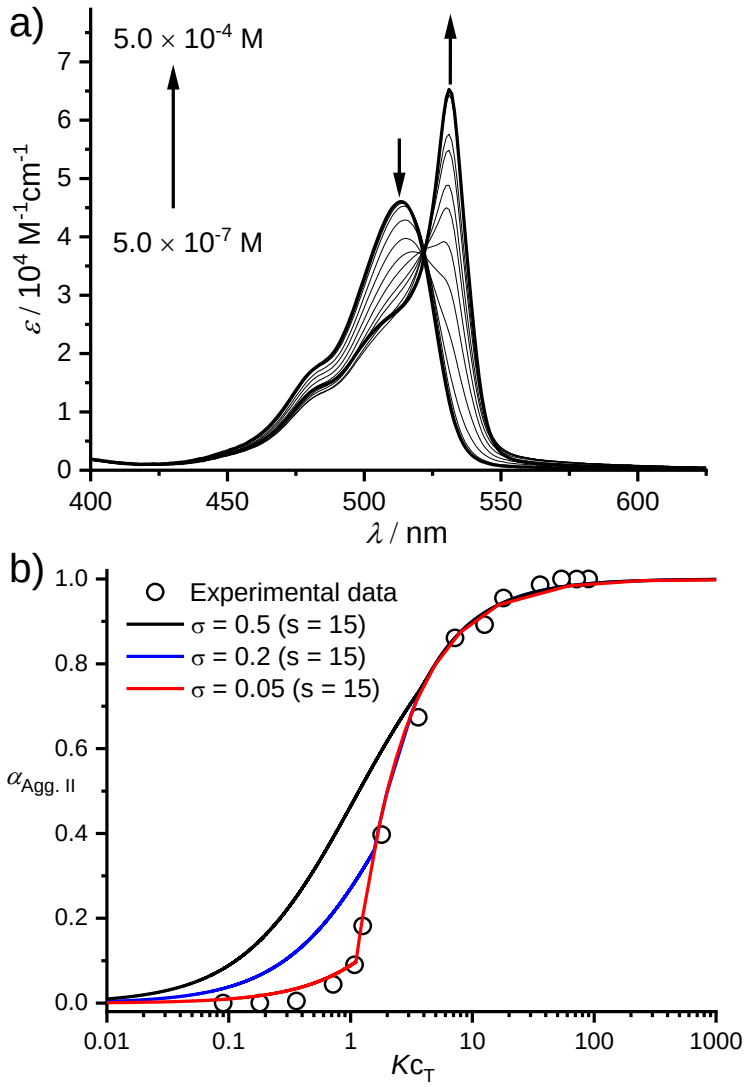

Fig. S11 a) Concentration-dependent UV/Vis absorption spectra of dye **3** in H_2O with concentration increasing from 5.0×10^{-7} M to 5.0×10^{-4} M. b) Plot of α_{agg} versus Kc_T with various σ and s values according to Goldstein and Stryer's model and the fitting of experimental data of dye **3** at 531 nm (circles) from concentration-dependent UV/Vis absorption spectra to the calculated curves.

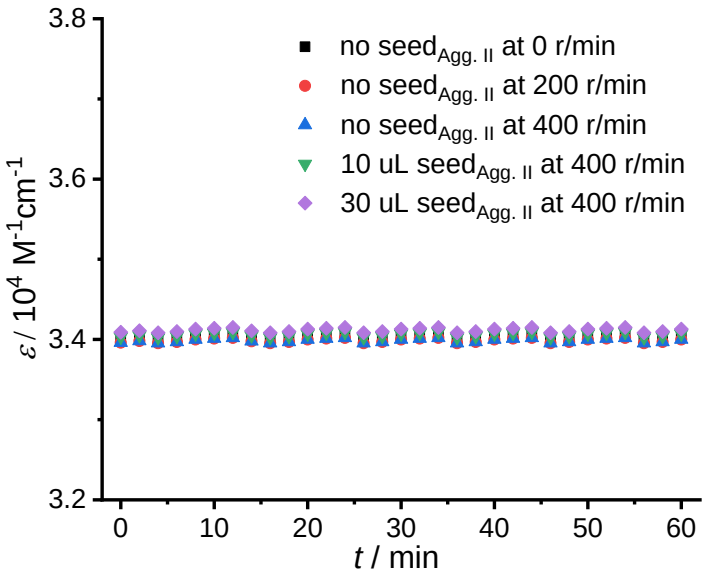

Fig. S12 Changes of the ε value at 531 nm in time-dependent UV/Vis absorption change of **Agg. I** in H_2O (c_T = 2.0 × 10^{-5} M) at 275 K under the different amount of seed$_{Agg.\ II}$ and stirring rate.

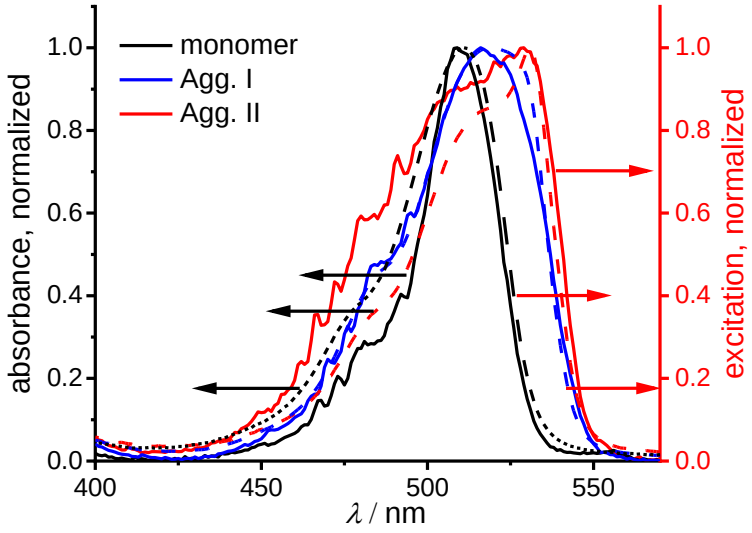

Fig. S13 Excitation spectra of monomer (c_T = 1.0 × 10^{-6} M, black solid line), and **Agg. I** (c_T = 1.0 × 10^{-5} M, blue solid line) and **Agg. II** (c_T = 1.0 × 10^{-5} M, red solid line) in H_2O (λ_{em} = 610 nm) compared to absorption spectra of monomer (c_T = 1.0 × 10^{-6} M, black dotted line), and **Agg. I** (c_T = 1.0 × 10^{-5} M, blue dotted line) and **Agg. II** (c_T = 1.0 × 10^{-5} M, red dotted line) in H_2O.

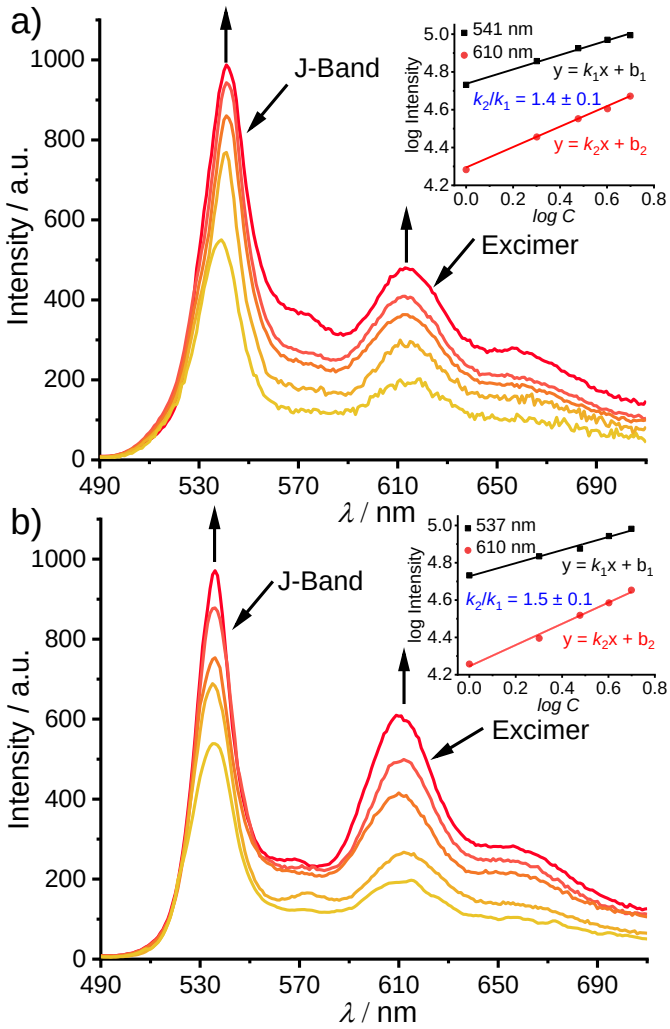

Fig. S14 a) Fluorescence intensity of **Agg. II** in H_2O with increasing concentration of the dye from 1.0×10^{-5} M to 5.0×10^{-5} M (λ_{ex} = 480 nm). Inset: Concentration-dependent of the emissive intensity of the excimer band (red symbol) and J-band (black symbol), and the solid lines were their linear fits. b) Fluorescence intensity of **Agg. I** in H_2O with increasing concentration of the dye from 1.0×10^{-5} M to 5.0×10^{-5} M (λ_{ex} = 480 nm). Inset: Concentration-dependent of the emissive intensity of the excimer band (red symbol) and J-band (black symbol), and the solid lines were their linear fits.

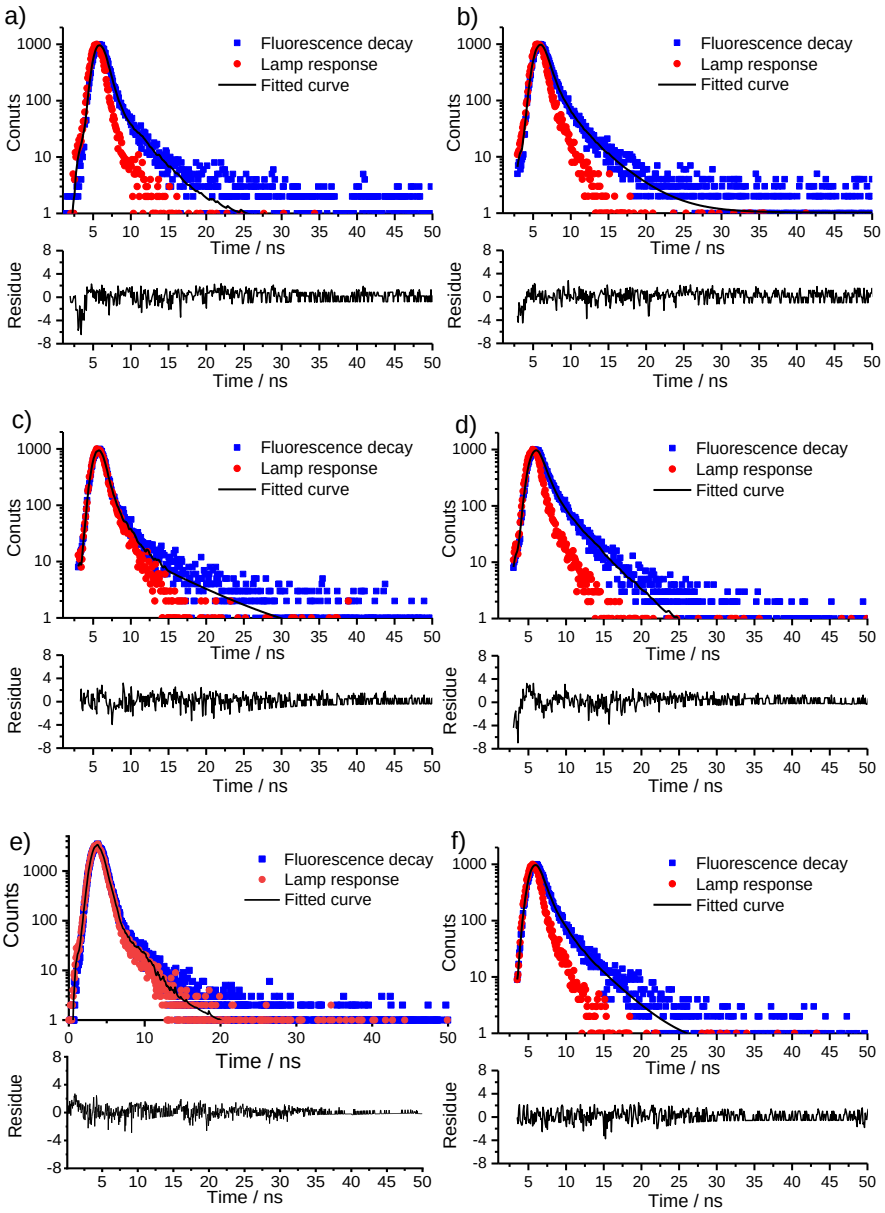

Fig. S15 a) Fluorescence decay of monomer of dye **3** in H_2O (c_T = 1.0 × 10^{-6} M, λ_{ex} = 366 nm, $\lambda_{detetion}$ = 530 nm) at 275 K. b) Fluorescence decay of monomer of dye **3** in H_2O (c_T = 1.0 × 10^{-6} M, λ_{ex} = 366 nm, $\lambda_{detetion}$ = 610 nm) at 275 K. c) Fluorescence decay of **Agg. I** of dye **3** in H_2O (c_T = 2.0 × 10^{-5} M, λ_{ex} = 366 nm, $\lambda_{detetion}$ = 537 nm) at 275 K. d) Fluorescence decay of **Agg. I** of dye **3** in H_2O (c_T = 2.0 × 10^{-5} M, λ_{ex} = 366 nm, $\lambda_{detetion}$ = 610 nm) at 275 K. e) Fluorescence decay of **Agg. II** of dye **3** in H_2O (c_T = 2.0 × 10^{-5} M, λ_{ex} = 366 nm, $\lambda_{detetion}$ = 541 nm) at 275 K. f) Fluorescence decay of **Agg. II** of dye **3** in H_2O (c_T = 2.0 × 10^{-5} M, λ_{ex} = 366 nm, $\lambda_{detetion}$ = 610 nm) at 275 K.

Table S1 Fluorescence lifetimes of dye **3** monomer, **Agg. I** and **Agg. II** in H_2O[a]

	τ_1 / ns (%)[b]	τ_2 / ns (%)[b]	τ / ns [c]	χ^2
Monomer	0.46 (85.17%)	3.01 (14.83%)	0.84	1.008
Agg. I	0.20 (96.19%)	6.50 (3.81%)	0.44	1.009
Agg. II	0.18 (98.02%)	5.43 (1.98%)	0.28	1.003

[a] Monitored at the emission maximum

[b] Components of bi-exponential fluorescence lifetimes and pre-exponential factors (in brackets)

[c] Averaged fluorescence lifetime

Table S2 Fluorescence lifetimes of excimer in H_2O[a]

	τ_1 / ns (%)[b]	τ_2 / ns (%)[b]	τ / ns [c]	χ^2
Monomer	0.57 (67.83%)	6.85 (32.17%)	2.6	1.027
Agg. I	0.64 (73.22%)	3.27 (26.78%)	1.3	1.019
Agg. II	0.55 (77.22%)	3.27 (22.78%)	1.1	1.004

[a] Monitored at 610 nm

[b] Components of bi-exponential fluorescence lifetimes and pre-exponential factors (in brackets)

[c] Averaged fluorescence lifetime

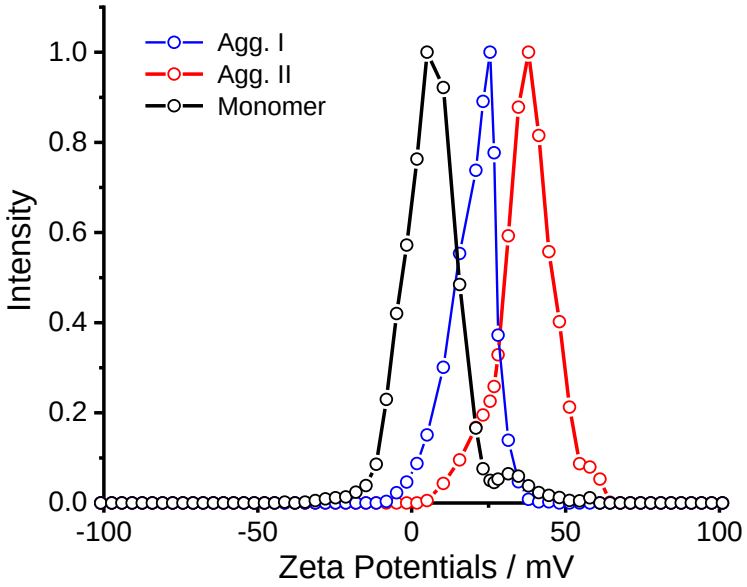

Fig. S16 Zeta Potentials of monomer, **Agg. I** and **Agg. II** in H_2O.

5. References

1. I. Botev, *Fresenius Z. Anal. Chem.*, 1979, **297**, 419-419.
2. P. Jonkheijm, P. van der Schoot, A. P. H. J. Schenning and E. W. Meijer, *Science*, 2006, **313**, 80-83.
3. R. F. Goldstein and L. Stryer, *Biophys. J.*, 1986, **50**, 583-599.
4. Z. Chen, Y. Liu, W. Wagner, V. Stepanenko, X. Ren, S. Ogi and F. Würthner, *Angew. Chem. Int. Ed.*, 2017, **56**, 5729-5733.